Maximum efficiency of absorption refrigerators at arbitrary cooling power

Zhuolin Ye[1,*] and Viktor Holubec[1,2,†]

[1]*Institut für Theoretische Physik, Universität Leipzig, Postfach 100 920, D-04009 Leipzig, Germany*
[2]*Charles University, Faculty of Mathematics and Physics, Department of Macromolecular Physics, V Holešovičkách 2, CZ-180 00 Praha, Czech Republic*

We consider absorption refrigerators consisting of simultaneously operating Carnot-type heat engine and refrigerator. Their maximum efficiency at given power (MEGP) is given by the product of MEGPs for the internal engine and refrigerator. The only subtlety of the derivation lies in the fact that the maximum cooling power of the absorption refrigerator is not limited just by the maximum power of the internal refrigerator, but, due to the first law, also by that of the internal engine. As a specific example, we consider the simultaneous absorption refrigerators composed of low-dissipation (LD) heat engines and refrigerators, for which the expressions for MEGPs are known. The derived expression for maximum efficiency implies bounds on the MEGP of LD absorption refrigerators. It also implies that a slight decrease in power of the absorption refrigerator from its maximum value results in a large nonlinear increase in efficiency, observed in heat engines, whenever the ratio of maximum powers of the internal engine and the refrigerator does not diverge. Otherwise, the increase in efficiency is linear as observed in LD refrigerators. Thus, in all practical situations, the efficiency of LD absorption refrigerators significantly increases when their cooling power is slightly decreased from its maximum.

I. INTRODUCTION

The performance of heat engines, transforming heat to work, or refrigerators and heat pumps, displacing heat against a temperature gradient, is determined by two main quantities: output power and efficiency. Unfortunately, thermodynamic laws imply that they cannot be optimized simultaneously [1]. This is because the largest efficiencies correspond to reversible and thus slow processes, leading to output powers which are at best negligible fractions of the maximum power [2].

The implication for engineers, whose natural task is to develop designs that deliver a desired (fixed) power as cheaply as possible, is that their devices in general do not operate in the regimes of maximum efficiency [1,3] or maximum power [4–21], which were both thoroughly investigated theoretically in the past, but rather in the regime with maximum efficiency corresponding to the given power (MEGP). The MEGP received the attention of the theory of finite-time thermodynamic processes only recently [22–27], generalizing results obtained previously for a variety of trade-off relations between power and efficiency [28–37].

Unlike model-independent equilibrium results such that the maximum efficiency of thermal devices is the Carnot efficiency [1,3], all available results on the optimal performance of thermal devices operating with finite cycle times are based on specific model systems. Nevertheless, these models are usually constructed in an idealized fashion so that real-world devices inevitably dissipate more and thus operate at smaller efficiencies. The results for MEGP obtained in these models thus represent (loose) upper bounds on real-world efficiencies.

Specifically, the idealized models just consider inevitable energy losses imposed by the second law of thermodynamics. In particular, losses connected to heat leakages and construction imperfections are neglected. Most of the idealized models operate along a finite-time Carnot cycle composed of two adiabatic and two isothermal branches and assume that the total entropy change in the universe during each of the isotherms obeys the so-called low-dissipation (LD) assumption [7]

$$\Delta S_{\text{tot}} = \Sigma/t, \tag{1}$$

where the irreversibility parameter $\Sigma > 0$ depends on details of the system construction, and t is the duration of the isotherm. The low-dissipation assumption is not just a useful approximation allowing to derive explicit analytical results. This model exactly describes Brownian heat engines optimized with respect to output power [15,24], which can now be realized in experiments [38,39]. More generally, the LD model describes the first finite-time correction to the quasistatic dissipation, which was revealed not only in theoretical studies [40–42], but also in experiments [39,43]. Furthermore, with respect to MEGP, the LD model was shown to be equivalent to the minimally nonlinear irreversible model [14,33,44], and, for small temperature gradients, also to the linear irreversible model [26]. Regardless of the relatively simple mathematical structure of the LD models, the exact results on MEGP are so far known for LD heat engines [25] and refrigerators [44] only. Other devices such as absorption refrigerators [45] and heat pumps [46] are still investigated numerically even when formulated within the LD setting.

*zhuolinye@foxmail.com
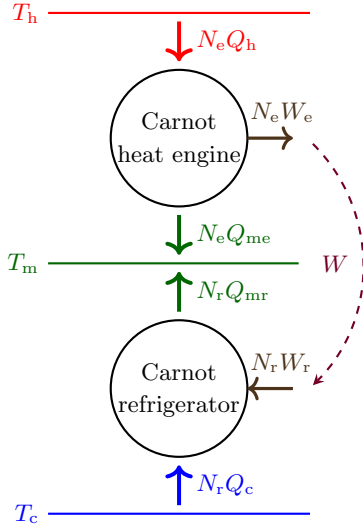†viktor.holubec@mff.cuni.cz

FIG. 1. Sketch of the CAR composed of internal Carnot heat engine and Carnot refrigerator. The overall CAR system communicates with three heat reservoirs at temperatures $T_h > T_m > T_c$. Both the internal engine and refrigerator use as their heat sink the reservoir at the intermediate temperature T_m. The engine in addition communicates with the hot bath at T_h and the refrigerator with the cold bath at T_c.

In the present paper, we consider absorption refrigerators consisting of simultaneously operating Carnot-type (internal) heat engine and refrigerator. We show how the MEGP for this general model follows from the MEGPs for the internal heat engine and refrigerator. To derive explicit results, we consider absorption refrigerators consisting of LD heat engines and refrigerators, for which expressions for MEGPs are known. The obtained MEGP represents a loose upper bound for the efficiency of real-world absorption refrigerators, which recently experienced a renewed interest of physicists due to their potential to recycle waste heat in microscopic (quantum) devices [47–52].

The rest of the paper is organized as follows. In Sec. II, we introduce the general model and derive the general results. In Sec. III, we derive the MEGP for LD absorption refrigerators and discuss its properties. We conclude in Sec. IV.

II. CARNOT ABSORPTION REFRIGERATORS

We consider absorption refrigerators consisting of a finite-time Carnot heat engine and refrigerator, which we call as Carnot absorption refrigerators (CARs). As shown in Fig. 1, the internal engine utilizes the temperature gradient $T_h - T_m > 0$ between a hot thermal reservoir and a thermal reservoir at a medium temperature to generate work. This work is then used to propel the internal refrigerator, which pumps heat from the cold thermal reservoir at temperature $T_c < T_m$ into the intermediate bath. As a result, the CAR utilizes heat from the hot body to further cool the cold one. In practice, such refrigerators are often used in cases where there is no reliable source of electricity, for example, in caravans. While described already in 1858 by Carré, absorption refrigerators now acquired renewed attention in the field of quantum thermodynamics [47–53]. This is because they seem to be promising

building blocks of quantum devices, where they should help to keep the quantum parts at very low temperatures by utilizing the junk heat produced by classical chips inevitably present in these setups.

In this work, we aim to provide an upper bound for MEGP for CARs and thus we assume that the internal engine and refrigerator work simultaneously [54]. Another possibility would be that they alternate [45]. Such CARs, however, involve during their operation idle periods of the internal devices and thus provide smaller MEGPs than the simultaneously operating setup. As we show below, the MEGP for simultaneous setups follows from MEGPs for the internal devices. In Appendix A, we discuss that for the alternating setup the optimization is actually more complicated and the knowledge of MEGPs of the internal engine and refrigerator is not sufficient for the derivation of MEGP.

A. Working cycle of simultaneous CAR

Below, we will optimize the efficiency of the CAR with respect to durations t_e and t_r of the engine and refrigeration cycles and thus we assume that they are different. The duration of one cycle of the CAR, t_s, is defined as a period after which both the internal devices attain their initial states. It is thus given by the least common multiple of t_e and t_r. We assume that such a common multiple exists and denote it as

$$N_e = t_s/t_e, \qquad (2)$$

($N_r = t_s/t_r$) the number of engine (refrigeration) cycles performed per one full CAR cycle.

Now we are ready to define the thermodynamic quantities of interest, sketched in Fig. 1. Per CAR cycle, the engine produces work $W = N_e W_e$, which is used by the refrigerator to pump heat $N_r Q_c$ from the cold bath. The output power of the engine W/t_s and the input power of the refrigerator thus reads

$$P \equiv W_e/t_e = W_r/t_r, \qquad (3)$$

where $W_r = W/N_r$ denotes the work used by the refrigerator per refrigeration cycle.

According to the first law, we have $W_e = Q_h - Q_{me}$ and $Q_c = Q_{mr} - W_r$. Here, Q_h and Q_{me} are the heats taken from the hot bath and delivered to the intermediate bath by the engine per period t_e, respectively. Similarly, Q_{mr} is heat pumped into the intermediate bath by the refrigerator per period t_r. The amount of heat extracted by the internal refrigerator from the cold bath per CAR cycle is given by $N_r Q_c$. The cooling powers of the simultaneous CAR R_s and the internal refrigerator R are thus the same and read

$$R_s = R = N_r Q_c/t_s = Q_c/t_r. \qquad (4)$$

The energy input of the CAR is $N_e Q_h$ and thus its efficiency, referred to as the coefficient of performance (COP), is given by

$$\psi = \frac{N_r Q_c}{N_e Q_h} = \frac{Q_c/t_r}{Q_h/t_e} = \varepsilon\eta. \qquad (5)$$

Here, $\eta = W_e/Q_h$ and $\varepsilon = Q_c/W_r = R/P$ denote the efficiency of the internal heat engine and refrigerator, respectively.

B. Maximum cooling power

Before we turn our attention to the MEGP for CARs, we determine the interval of allowed values of the cooling power (4). Its minimum value 0 is achieved for infinitely slow cycles. The maximum cooling power R_s^* turns out to be limited by maximum powers of both constituting devices.

The power source of the refrigerator inside the CAR is the internal heat engine and thus the maximum cooling power of the CAR cannot be larger than the maximum cooling power of the internal refrigerator without restrictions to input power R^*, i.e., $R_s^* \leqslant R^*$. Furthermore, the cooling power is related to output power of the engine by

$$P = R/\varepsilon(R). \tag{6}$$

We denote as $\bar{R}$ the maximum value of cooling power solving the equation

$$P^* = \bar{R}/\varepsilon(\bar{R}), \tag{7}$$

where P^* is the maximum power of the engine. If $\bar{R} < R^*$, the engine is not powerful enough to utilize the whole potential of the refrigerator and $R_s^* = \bar{R}$. Similarly, $\bar{R} > R^*$ means that the refrigerator is not powerful enough to use the enitre power provided by the engine and $R_s^* = R^*$. Altogether, we found that the maximum power of the CAR is given by

$$R_s^* = \min(\bar{R}, R^*). \tag{8}$$

In the next section, we finally discuss the MEGP for the simultaneous CARs.

C. MEGP for simultaneous CARs

Inserting Eq. (6) for engine output power as function of power of the refrigerator in Eq. (5), we obtain the COP of the CAR as function of R:

$$\psi(R) = \varepsilon(R)\eta\left[\frac{R}{\varepsilon(R)}\right]. \tag{9}$$

To get the MEGP for CAR, we need to optimize the right-hand side of this equation with respect to the durations of t_r and t_e for fixed R. Using Eqs. (6), (B2), and (C1), Eq. (9) can be rewritten in the form

$$\psi(R) = \frac{\eta_C \varepsilon_C}{1 + \varepsilon_C T_m \sigma/R}, \tag{10}$$

where η_C and ε_C are the Carnot efficiency of reversible Carnot heat engine and refrigerator, respectively, i.e., $\eta_C = 1 - T_m/T_h$ and $\varepsilon_C = T_c/(T_m - T_c)$, and

$$\sigma = \Delta S_{\text{tot,r}}/t_r + \Delta S_{\text{tot,e}}/t_e \tag{11}$$

is the sum of the average entropy production rates in the internal heat engine and internal refrigerator and thus the total average entropy production rate during the CAR cycle. Expressions for the total entropy changes per engine and refrigeration cycle $\Delta S_{\text{tot},r}$ and $\Delta S_{\text{tot},e}$ are given in Eqs. (B3) and (C2) in the Appendix. The maximization of COP (9) at fixed R is thus equivalent to the minimization of the average entropy production rate $\sigma = \sigma(R)$ under the same conditions.

The output power of the internal heat engine depends on the setup and performance of the refrigerator through the refrigeration power $R/\varepsilon(R)$ only. Thus, to yield the maximum value of the product in Eq. (9), $\eta[R/\varepsilon(R)]$ must attain its maximal value, $\eta^{\text{opt}}[R/\varepsilon(R)]$, corresponding to the given refrigeration power (MEGP). Furthermore, all known expressions for MEGP are decreasing functions of power [25,26,44,55,56]. Importantly, all these models neglect losses, which cannot be avoided by quasistatic operation, such as heat leakages, and thus they can saturate the Carnot bound on efficiency in the limit of vanishing power. Assuming that this idealization holds also in our present case, $\eta^{\text{opt}}[R/\varepsilon(R)]$ will be maximal if $\varepsilon(R)$ will be given by the maximum refrigerating efficiency at the given power $\varepsilon^{\text{opt}}(R)$. Altogether, the MEGP for the considered idealized CARs reads

$$\psi^{\text{opt}}(R) = \varepsilon^{\text{opt}}(R)\eta^{\text{opt}}\left[\frac{R}{\varepsilon^{\text{opt}}(R)}\right]. \tag{12}$$

The MEGP for the simultaneous CAR thus, in general, follows from the expressions for MEGPs for the internal engine and refrigerator. Let us now consider the simultaneous CAR composed of a LD heat engine and LD refrigerator [25,44]. For this specific model, we verified the validity of Eq. (12) by direct numerical maximization of Eq. (9). In the next section, we utilize the known analytical expressions for η^{opt} and ε^{opt} for this model to discuss in detail properties of the MEGP (12) for this LD CAR based on analytical grounds.

III. LOW-DISSIPATION SIMULTANEOUS CARS

Let us now consider the Carnot LD heat engine and refrigerator depicted in Fig. 2, for which the MEGPs were derived in Refs. [25] and [44], respectively. Their working cycles are composed of two isotherms realized in finite time and described by the irreversibility parameters Σ_i, $i = h, me, c, mr$. These isotherms are interconnected by infinitely fast adiabats [57].

The internal engine accepts heat

$$Q_h = T_h \Delta S_e - \frac{\Sigma_h}{t_h} \tag{13}$$

during the hot isotherm (red) of duration t_h and releases heat

$$Q_{me} = T_m \Delta S_e + \frac{\Sigma_{me}}{t_{me}} \tag{14}$$

during the isotherm corresponding to the medium temperature (green) of duration t_{me}. The terms proportional to the increase in the entropy of the working medium of the engine during the hot isotherm, ΔS_e, correspond to the reversible parts of the transferred heats. The total duration of the engine working cycle reads $t_e = t_h + t_{me}$. Similarly, the refrigerator accepts heat

$$Q_c = T_c \Delta S_r - \frac{\Sigma_c}{t_c} \tag{15}$$

during the cold isotherm (blue) of duration t_c and dumps heat

$$Q_{mr} = T_m \Delta S_r + \frac{\Sigma_{mr}}{t_{mr}} \tag{16}$$

during the intermediate isotherm (green) of duration t_{mr}. The reversible components of transferred heats are proportional to the increase in the entropy of the working medium of the
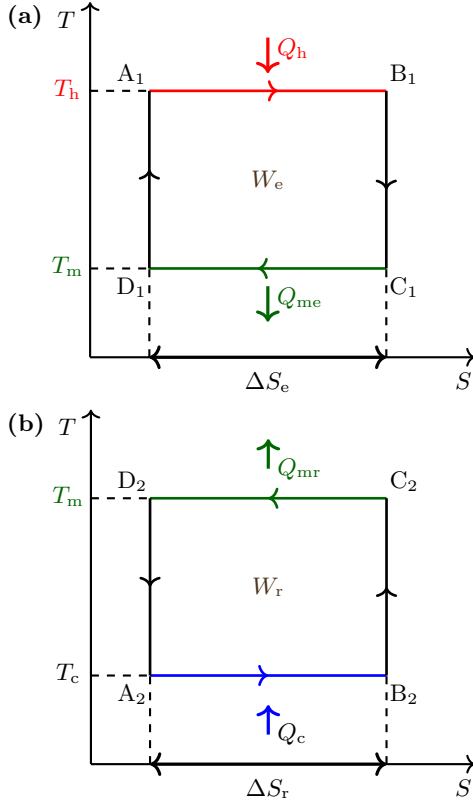
FIG. 2. Bath temperature-system entropy (T-S) diagrams of the components of the CAR depicted in Fig. 1 considered in its low-dissipation version. (a) LD Carnot heat engine and (b) LD Carnot refrigerator. The horizontal colored lines are isotherms and the vertical black lines represent adiabats. The areas enclosed of the two rectangles equal to the respective works only if the cycles are realized quasistatically.

refrigerator during the cold isotherm ΔS_r, which can be different than ΔS_e. The total duration of the refrigeration cycle is $t_r = t_c + t_{mr}$. The internal heat engine and refrigerator operate reversibly if the duration of all the isotherms diverge or if all the irreversibility parameters vanish.

Let us now consider a simultaneous CAR composed of the LD heat engine and LD refrigerator. We call it an LD simultaneous CAR. In what follows, we discuss in detail its performance in terms of MEGP.

A. MEGP

The MEGP for the LD CAR follows from Eq. (12) after inserting the expressions for MEGP of the internal LD heat engine η^{opt} and refrigerator ε^{opt}. For the engine, we derive η^{opt} in Appendix B. Similarly to the derivation given in Ref. [25], our present approach involves an approximation in calculation of the optimal redistribution of the total cycle duration between the two isothermal branches. Nevertheless, our analytical result for η^{opt} is, within the numerical precision, indistinguishable from the corresponding result obtained by exact numerical optimization of the efficiency. For the refrigerator, we review in Appendix C the derivation of analytical expression for ε^{opt} from Ref. [44].

All results for MEGP available in the literature [2,24–26,44,55,56] are given as functions of the dimensionless variable

$$\delta X = \frac{X - X^*}{X^*}, \tag{17}$$

measuring how much power is lost by operating the device at power X smaller than the maximum power X^*. In our case, we have three such variables: the loss in power of the internal engine δP; the loss in cooling power of the internal refrigerator δR; and the loss in cooling power of the CAR δR_s. In general, these variables can assume values from the interval $[-1, 0]$. The minimum is attained if the actual power is negligible compared to the maximum power and the maximum corresponds to devices operating at maximum power. However, in our specific setting where the input power of the refrigerator can be limited by the output power of the engine, the upper bound for δR reads $R_s^*/R^* - 1 \leqslant 0$.

To insert the known results for MEGP of the refrigerator and heat engine into Eq. (12), we need to express them in terms of refrigeration power R and engine output power $P = R/\varepsilon^{\text{opt}}(R)$, respectively. From now on, we use the shorthand notation $\varepsilon^{\text{opt}}(\delta R) \equiv \varepsilon^{\text{opt}}[R(\delta R)]$, where $R(\delta R) = (1 + \delta R)R^*$, and similarly for $\eta^{\text{opt}}(\delta P)$. Furthermore, to be able to discuss the MEGP of the CAR, $\psi^{\text{opt}} = \varepsilon^{\text{opt}}(\delta R)\eta^{\text{opt}}(\delta P)$, as a function of the loss in cooling power of the CAR, we use Eqs. (6) and (17) to express δP and δR in terms of δR_s. The result is

$$\delta P = \frac{1}{\tilde{P}^*} \frac{1 + \delta R}{\varepsilon^{\text{opt}}(\delta R)} - 1, \tag{18}$$

$$\delta R = (1 + \delta R_s)\tilde{R}_s^* - 1, \tag{19}$$

where we introduced the reduced maximum powers of the engine $\tilde{P}^* = P^*/R^*$, and the CAR, $\tilde{R}_s^* = R_s^*/R^*$, measured in units of maximum power of the internal refrigerator.

When expressed in terms of δP, the MEGP of the LD heat engine η^{opt} depends only on the ratio of the irreversibility parameters $\Sigma_e = \Sigma_h/\Sigma_{me}$, Carnot efficiency, η_C, and δP. For details, see Appendix B. Similarly, we show in Appendix C that ε^{opt} is only a function of $\Sigma_r = \Sigma_{mr}/\Sigma_c$, $\varepsilon_C = T_c/(T_m - T_c)$ and δR. Since the MEGP $\varepsilon^{\text{opt}}(R)$ is a monotonously decreasing function of R, the ratio $R/\varepsilon^{\text{opt}}(R)$ attains its maximum value for R^*. Therefore, Eqs. (7) and (8) imply that the reduced maximum power of the CAR $\tilde{R}_s^*$ is given by

$$\tilde{P}^* = \tilde{R}_s^*/\varepsilon^{\text{opt}}(\tilde{R}_s^* - 1) \tag{20}$$

if the resulting $\tilde{R}_s^*$ is smaller than 1 and by $\tilde{R}_s^* = 1$ otherwise. Hence $\tilde{R}_s^*$ is determined by Σ_r, ε_C, and $\tilde{P}^*$. Collecting all these results and inserting them into Eq. (12), we can finally write the MEGP of the LD simultaneous CAR in terms of the relative loss in its maximum cooling power δR_s. The resulting expression depends on the six parameters introduced above, namely,

$$\psi^{\text{opt}} \equiv \psi^{\text{opt}}(\delta R_s, \tilde{P}^*, \Sigma_e, \Sigma_r, \eta_C, \varepsilon_C). \tag{21}$$

In the following sections, we use this expression to provide more explicit results on MEGP of CARs.

B. Bounds on MEGP

We start by deriving maximum and minimum values of the optimal COP ψ^{opt} with respect to the working medium of the CAR (or of its constituents). In the LD approximation, the detailed physics of the working medium is described by the irreversibility parameters Σ_i, $i = h, me, c, mr$ defined by Eqs. (13) to (16) [15,24,40,58,59].

The optimal COP (21) depends on irreversibility parameters through the ratios $\Sigma_e = \Sigma_h/\Sigma_{me}$ and $\Sigma_r = \Sigma_{mr}/\Sigma_c$ and the reduced maximum power of the internal engine $\tilde{P}^*$. With respect to the previous two, the optimal COP attains its minimum for $\Sigma_e \to 0$ (hot isotherm of the internal engine cycle is reversible compared to the other one) and $\Sigma_r \to \infty$ (cold isotherm of the refrigeration cycle is reversible compared to the other one). Its maximum ψ^{opt} is attained in the opposite limit $\Sigma_e \to \infty$ and $\Sigma_r \to 0$. Taking these limits into Eq. (21), we find the lower and upper bounds for the optimal COP as follows:

$$0 \leqslant \psi^{\mathrm{opt}} \leqslant \frac{\varepsilon_C(1 + \sqrt{-\delta R})}{2 + \varepsilon_C(1 - \sqrt{-\delta R})} \frac{\eta_C(1 + \sqrt{-\delta P})}{2 - \eta_C(1 - \sqrt{-\delta P})}. \quad (22)$$

This inequality has to be further optimized with respect to the parameter $\tilde{P}^*$, which enters the upper bound through Eqs. (18) and (19) for δP and δR, respectively. Note that, due to the limits $\Sigma_e \to \infty$ and $\Sigma_r \to 0$ taken to derive the upper bound, we have to use $\varepsilon^{\mathrm{opt}} = \varepsilon_+^{\mathrm{opt}}$ defined in Eq. (C13) in the formula for δP. One finds that the upper bound is a monotonously decreasing function of $\tilde{P}^*$ and thus its maximum is obtained for $\tilde{P}^* = 0$. The resulting ultimate bounds on the optimal COP of the CAR at given cooling power read

$$0 \leqslant \psi^{\mathrm{opt}} \leqslant \frac{\varepsilon_C \eta_C(1 + \sqrt{-\delta R_s})}{2 - \eta_C(1 - \sqrt{-\delta R_s})} \equiv \psi_+^{\mathrm{opt}}(\delta R_s). \quad (23)$$

The upper bound evaluated for $\delta R_s = 0$, $\psi_+^{\mathrm{opt}}(0) = \varepsilon_C \eta_C/(2 - \eta_C)$, denotes the upper bound for COP of the CAR at maximum cooling power.

The increase in COP gained after a slight decrease of the cooling power from its maximum value can be measured by the expression

$$\frac{\psi_+^{\mathrm{opt}}(\delta R_s) - \psi_+^{\mathrm{opt}}(0)}{\psi_+^{\mathrm{opt}}(0)} = \frac{2 - 2\eta_C}{2 - \eta_C} \sqrt{-\delta R_s} + \mathcal{O}(\delta R_s). \quad (24)$$

Its derivative with respect to δR_s diverges, implying that a slight decrease of the cooling power leads to a significant gain in the upper bound on COP. Qualitatively the same behavior has generally been observed for MEGPs of various heat engines [22,23,25–27,56]. With respect to LD refrigerators, the MEGP is proportional to $\sqrt{-\delta R}$ for a limited range of parameters only and behaves as $\propto -\delta R$ otherwise [44]. In the next section, we investigate whether the increase of MEGP for the CAR behaves for small values of δR_s always like MEGPs in heat engines [25] or if it sometimes also exhibits the linear behavior observed in refrigerators [44].

C. MEGP near maximum cooling power

Examples of parameter regimes where the MEGP for LD refrigerators exhibits the two qualitatively different behaviors are $\Sigma_r \to 0$ (square root) and $\Sigma_r \to \infty$ (linear) [44]. We thus investigate behavior of the MEGP for the CAR (21) in these two regimes using the cumbersome analytical expressions derived in Appendixes B and C.

1. $\Sigma_r \to 0$

Expanding the exact expression for $\varepsilon^{\mathrm{opt}}$ in Eq. (C12) up to the first order with respect to Σ_r, we obtain

$$\varepsilon^{\mathrm{opt}} = \varepsilon_+^{\mathrm{opt}} - \frac{2(1 + \varepsilon_C)\left(\varepsilon_+^{\mathrm{opt}}\right)^2(1 - \sqrt{-\delta R})\sqrt{\tilde{\Sigma}_r}}{\varepsilon_C(-\delta R)^{1/4}(1 + \sqrt{-\delta R})}, \quad (25)$$

where $\tilde{\Sigma}_r$ is defined below Eq. (C11) and $\varepsilon_+^{\mathrm{opt}}$ in Eq. (C13). Substituting Eqs. (25) and (B14) for $\varepsilon^{\mathrm{opt}}$ and η^{opt} into Eq. (12) for MEGP for the CAR, expressing δP and δR in terms of δR_s using Eqs. (18) and (19), and expanding the resulting expression up to the first order in δR_s, we find

$$\psi^{\mathrm{opt}} = r_1 + r_2\sqrt{-\delta R_s}. \quad (26)$$

The coefficients r_1 and r_2 depend, in a complicated way, on the parameters $\tilde{P}^*$, ε_C, η_C, and Σ_e. The obtained dependence of the MEGP of the CAR on the loss in cooling power might have been expected since, in this parameter regime, the behavior near maximum power of the engine and the refrigerator is the same [25,44].

2. $\Sigma_r \to \infty$

In this limit, the MEGP for LD refrigerators (C12) reads (see Eq. (29) in Ref. [44])

$$\varepsilon^{\mathrm{opt}} \approx \frac{\delta R(1 - \delta R)\varepsilon_C}{2\delta R + (1 + \delta R)(\delta R - \Sigma_r)\varepsilon_C}. \quad (27)$$

Using a similar procedure as for obtaining Eq. (26), we find that up to the second order in δR_s

$$\psi^{\mathrm{opt}} = g_1 + g_2\sqrt{-\delta R_s} + g_3\delta R_s, \quad (28)$$

where the coefficients g_1, g_2, and g_3 depend on $\tilde{P}^*$, ε_C, η_C, and Σ_e in a complicated way. Interestingly, for $\tilde{P}^* \to \infty$, g_2 vanishes and the increase in COP of the CAR becomes linear. As discussed at the end of the next section, for diverging $\tilde{P}^*$, the heat engine works at Carnot efficiency and the behavior of the MEGP of the CAR is solely determined by that of the refrigerator [44].

D. MEGP for arbitrary parameters

Outside the limiting parameter regimes discussed above, the full analytical expression (21) for the MEGP is too cumbersome to get an immediate insight into the behavior of ψ^{opt}. Therefore, in this section, we investigate its dependence on the model parameters graphically.

In Fig. 3, we show the reduced maximum power of the CAR $\tilde{R}_s^*$ as a function of the reduced power of the internal heat engine $\tilde{P}^*$. The larger the available input power of the refrigerator (provided by the engine) the larger the corresponding maximum cooling power of the CAR until it reaches its maximum $\tilde{R}_s^* = 1$, where the whole cooling potential of the internal refrigerator is utilized. The minimum value of the reduced power $\tilde{P}^* = 1/\varepsilon^{\mathrm{opt}}(0)$, allowing for $\tilde{R}_s^* = 1$, follows from Eq. (20). Here, $\varepsilon^{\mathrm{opt}}(0) = \varepsilon_\pm^*$ denotes the MEGP for the
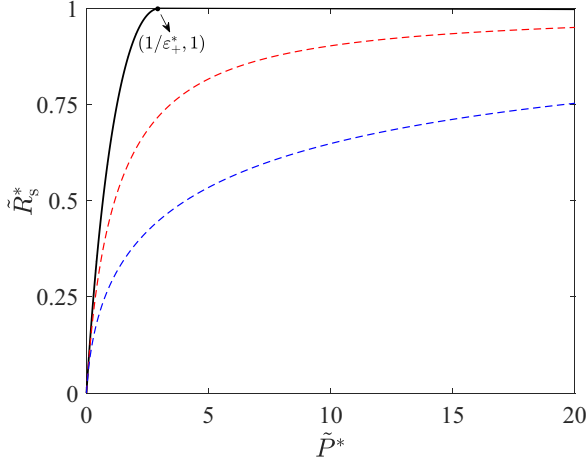
FIG. 3. The reduced maximum power of the CAR $\tilde{R}_s^*$ as a function of the reduced maximum power of the internal heat engine $\tilde{P}^*$ for three values 0, 1, and 10 of the ratio Σ_r of irreversibility parameters, which increases from the uppermost solid line to the lowermost dashed one. We take $\varepsilon_C = 1$.

refrigerator defined in Eqs. (C5) and (C6). Hence, $\tilde{R}_s^* = 1$ for finite value ($\tilde{P}^* = 1/\varepsilon_+^*$) of the reduced power only if $\Sigma_r = 0$, i.e., when the dissipation during the hot isotherm of the refrigeration cycle becomes negligible compared to that during the cold one. For $\Sigma_r > 0$, the whole cooling potential of the internal refrigerator can be utilized only for infinite values of the reduced power $\tilde{P}^* = 1/\varepsilon_-^* \to \infty$. This is caused by the discontinuity in the ability of the refrigerator working at maximum power conditions to utilize the energy provided by the engine $\varepsilon^{\mathrm{opt}}(0)$, which is positive for $\Sigma_r = 0$ and vanishes for $\Sigma_r > 0$ [44]. Figure 3 also shows that, for fixed $\tilde{P}^*$ and ε_C, $\tilde{R}_s^*$ decreases as the amount of energy dissipated during the hot isotherm of the refrigeration cycle increases (larger Σ_r).

In Fig. 4, we plot the MEGP for CARs (21) as a function of δR_s for different values of $\tilde{P}^*$, Σ_e, and Σ_r. The upper bounds (22) for MEGP for fixed reduced power $\tilde{P}^*$ are depicted for $\tilde{P}^* = 1$ (top pink solid line in the middle) and $\tilde{P}^* \geqslant 1/\varepsilon_+^*$ (bottom pink solid line in the middle). They indeed bound the MEGP obtained for arbitrary values of ratios of irreversibility parameters Σ_e and Σ_r, and values of $\tilde{P}^*$ larger than those chosen to plot the individual curves. The ultimate upper bound on MEGP (23) is depicted by the uppermost black solid line. According to the figure, the MEGP ψ^{opt} exhibits a fast nonlinear increase with decreasing power near $\delta R_s \to 0$ unless $\tilde{P}^* \to \infty$. Only then is this increase linear, in agreement with our discussion below Eq. (28). To check our analytical results, we also calculated the MEGP for simultaneous LD CARs by a direct brute-force numerical optimization of COP (5). The figure shows that the obtained numerical results (symbols) perfectly overlap with our analytical predictions (lines).

In Fig. 5, we show the characteristics of the heat engine and refrigerator corresponding to the MEGP of the CAR with $\Sigma_r = \Sigma_e = 1$, depicted in Fig. 4. For $\tilde{P}^* \to 0$, Eqs. (18) to (20) imply that $\delta R = -1$, $\varepsilon^{\mathrm{opt}} = \varepsilon_C$, and $\delta P = \delta R_s$. Similarly, for $\tilde{P}^* \to \infty$ it follows that $\delta R = \delta R_s$, $\delta P = -1$, and $\eta^{\mathrm{opt}} = \eta_C$. When the refrigerator works at the Carnot COP ε_C, the dimensionless refrigeration cycle duration τ_r^{opt} diverges and
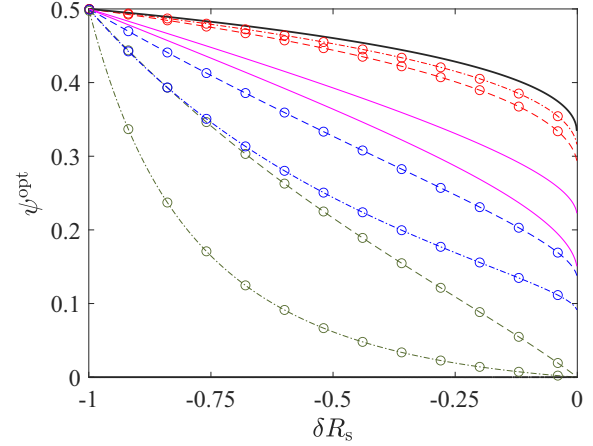

FIG. 4. The MEGP of the CAR (21) as a function of the loss in cooling power δR_s for three values 0, 1, and ∞ of the reduced maximum power of the engine $\tilde{P}^*$. The reduced power $\tilde{P}^*$ increases from the uppermost dashed line to the lowermost one with $\Sigma_r = \Sigma_e = 1$. The dot-dashed lines of the same color as the dashed ones correspond to the same $\tilde{P}^*$ and $\Sigma_r = \Sigma_e = 10$. The two pink solid lines in the middle depict the upper bound on MEGP (22) for fixed $\tilde{P}^*$ obtained for $\Sigma_r = 0$ and $\Sigma_e \to \infty$. For the top one we took $\tilde{P}^* = 1$. The bottom one corresponds to arbitrary $\tilde{P}^* \geqslant 1/\varepsilon_+^*$. The bottom and top black solid lines represent the ultimate lower ($\Sigma_r \to \infty$, $\Sigma_e = 0$, and arbitrary $\tilde{P}^*$) and upper ($\Sigma_r = 0$, $\Sigma_e \to \infty$, and $\tilde{P}^* = 0$) bounds on MEGP (23) (note that the lower bound coincides with the horizontal axis). MEGP for the CAR obtained using brute-force numerical optimization of its COP (circles) perfectly agree with the curves calculated using the analytical formula (21) (lines). Other parameters taken: $\varepsilon_C = 1$ and $\eta_C = 1/2$.

we have $N_e/N_r \to \infty$, i.e., within one full CAR cycle, there are infinitely more engine cycles than refrigeration cycles. An opposite situation occurs when the engine works at Carnot efficiency.

IV. CONCLUSION AND OUTLOOK

We showed that the maximum efficiency at given cooling power (MEGP) for an absorption refrigerator composed of simultaneously operating Carnot-type heat engine and Carnot-type refrigerator (CAR) follows from the MEGPs for the internal heat engine and refrigerator. We applied these general findings to low-dissipation (LD) simultaneous CARs, where the internal devices work in the LD regime and the corresponding expressions for MEGPs are known [25,44]. We used the resulting cumbersome analytical formula for the MEGP for derivation of concise expressions for upper and lower bounds on the MEGP for the LD CARs. We also investigated the behavior of the MEGP close to the maximum power. Unless the ratio of maximum powers of the internal engine and the refrigerator diverges, a slight decrease in power of the LD CAR leads to a fast nonlinear increase in the MEGP generically observed in heat engines [25]. Otherwise, the increase in the MEGP is linear as can be observed in LD refrigerators [44].

In the LD approximation, the detailed dynamics of the system in question determines the so-called irreversibility
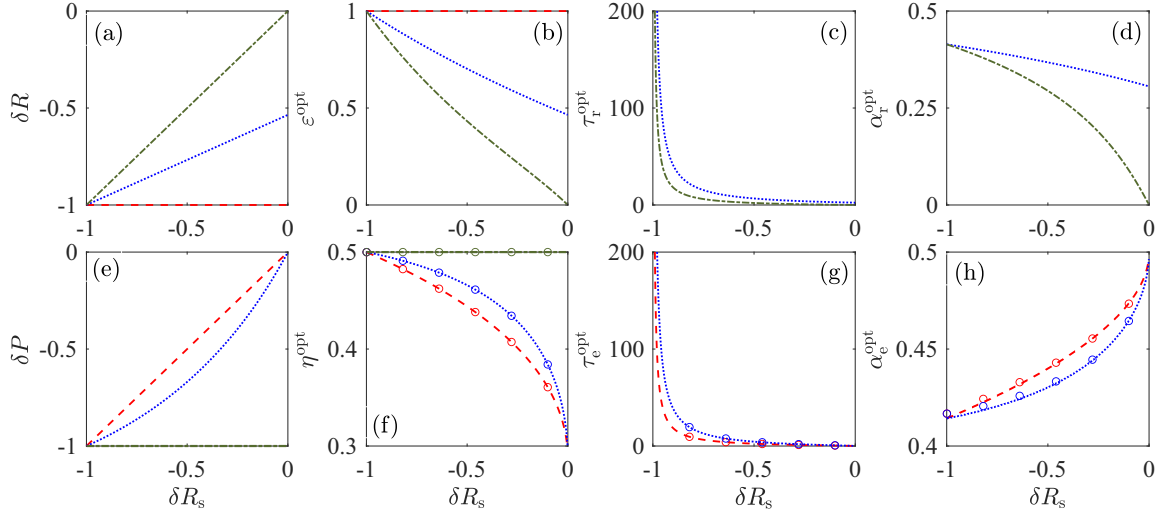
FIG. 5. Top: Characteristics of the internal refrigerator corresponding to the MEGP for the CAR depicted in Fig. 4 for $\Sigma_r = \Sigma_e = 1$ as functions of the loss in output power of the CAR, δR_s. (a) The loss in output power δR, (b) MEGP $\varepsilon^{\mathrm{opt}}$, (c) the optimal dimensionless cycle duration τ_r^{opt}, defined in Eq. (C7), and (d) the optimal relative duration of the hot isotherm α_r^{opt}, defined below Eq. (C7). Bottom: The corresponding characteristics of the internal heat engine. (e) The loss in output power δP, (f) MEGP η^{opt}, (g) the optimal dimensionless cycle duration τ_e^{opt} defined in Eq. (B8), and (h) the optimal relative duration of the hot isotherm α_e^{opt}, defined above Eq. (B1). Colors of the individual lines, marking the used value of the reduced maximum power $\tilde{P}^*$, are the same as those used in Fig. 4 (red dashed, blue dotted, green dash-dotted corresponds to reduced powers 0, 1, and ∞, respectively). The vanishing reduced power corresponds to the Carnot COP of the refrigerator $\varepsilon^{\mathrm{opt}} = \varepsilon_C$, where τ_r^{opt} diverges, and arbitrary α_r^{opt}. Panels (c) and (d) thus show no red dashed lines. Similarly, diverging $\tilde{P}^*$ corresponds to the Carnot efficiency of the engine $\eta^{\mathrm{opt}} = \eta_C$, and thus we show no green dash-dotted lines in panels (g) and (h). Even though the depicted parameters for the heat engines were obtained using the approximation (B13), they are almost indistinguishable from exact numerical results (circles). Slight deviations can be observed for α_e^{opt} only.

parameters. The MEGP for simultaneous LD CARs, derived in this paper, is as function of power measured in units of the maximum power, which depends on the irreversibility parameters. Using a specific dynamical model, the maximum power can be further optimized with respect to theses parameters, allowing to derive expressions for maximum power at fixed maximum efficiency. For LD heat engines and refrigerators, such an optimization was performed in Refs. [58,59] using the geometrical approach to thermodynamics generically valid close to equilibrium. While the dependence of maximum power on irreversibility parameters in these two settings is obvious, the situation in LD CARs is slightly different since their maximum power is controlled by both the maximum power of the internal refrigerator and that of the internal heat engine. Equations (7) and (8) suggest that the power of the CAR attains its maximum if one maximizes the COP of the internal refrigerator, its maximum power, and also the maximum power of the heat engine. However, detailed investigations in this direction will be a subject of our future work.

The presented LD model is constructed in an idealized fashion and the resulting MEGP can serve as a (loose) upper bound for real-world absorption refrigerators. Such bounds are thus nowadays available for heat engines [25], refrigerators [44], and absorption refrigerators. It remains to derive them for heat pumps, which will also be a subject of our future work. For a numerical study of the MEGP for absorption heat pumps, we refer to Ref. [46]. Furthermore, it would be interesting to investigate MEGPs for LD systems in context of the stability analysis described in Refs. [8,60–62].

Originally, the finite-time performance of heat engines was studied using the endoreversible model [63]. While efficiencies at maximum power for the endoreversible and LD models are described by similar expressions [64], to the best of our knowledge, no results for MEGP for endoreversible models are known. As a future research project, it would be also interesting to investigate to what extent the apparent equivalence between the two models holds concerning the MEGP.

APPENDIX A: MEGP FOR ALTERNATING CARS

For alternating CARs [45], the internal heat engine and refrigerator do not operate simultaneously. The duration of one cycle of the alternating CAR is thus given by the sum $t_e + t_r$ of the durations of the engine and refrigerator. According to the first law of thermodynamics, the output work of the heat engine per cycle equals to the input work of the refrigerator,

i.e., $W_e = W_r$. The power of the heat engine and the cooling power of the refrigerator then read

$$\mathcal{P} = \frac{W_e}{t_e + t_r} = \frac{P}{1 + \Lambda}, \quad \text{(A1)}$$

$$\mathcal{R} = \frac{Q_c}{t_e + t_r} = \frac{R}{1 + 1/\Lambda}, \quad \text{(A2)}$$

where $\Lambda \equiv t_r/t_e$ measures the ratio of durations of the two internal cycles. The first law in the form of Eq. (6) implies that these two powers are interconnected through the COP ε of the refrigerator

$$\mathcal{P} = \frac{\mathcal{R}}{\varepsilon(R)}. \quad \text{(A3)}$$

Using Eqs. (A2) and (A3), the COP (5) can be rewritten as

$$
\begin{aligned}
\psi(\mathcal{R}) &= \varepsilon(R)\eta(P) \\
&= \varepsilon(\mathcal{R}, \Lambda)\eta(\mathcal{P}, \Lambda) \\
&= \varepsilon(\mathcal{R}, \Lambda)\eta\left(\frac{\mathcal{R}}{\varepsilon(\mathcal{R}, \Lambda)}, \Lambda\right),
\end{aligned}
\quad \text{(A4)}
$$

where the notation $\varepsilon(R) = \varepsilon[\mathcal{R}(1 + 1/\Lambda)] \equiv \varepsilon(\mathcal{R}, \Lambda)$ highlights that both the efficiencies now explicitly depend on the ratio of the durations of the internal cycles Λ through the definitions (A1) and (A2) of $\mathcal{R}$ and $\mathcal{P}$. Consequently, in the optimization of COP (A4) with respect to the durations of the refrigeration and engine cycles, the engine and refrigeration efficiencies cannot be optimized independently as it was done in Eq. (12). The optimization of COP for alternating CARs is thus more complicated than that for simultaneous CARs and the knowledge of MEGPs for the internal engine and refrigerator might not be sufficient for determination of MEGP for alternating CARs.

APPENDIX B: MEGP FOR LD HEAT ENGINES

In this Appendix, we derive the expression η^{opt} for MEGP for LD heat engines. The derivation is slightly different from that used in Ref. [25].

Introducing the relative duration of the hot isotherm, $\alpha_e = t_h/t_e$, in Eqs. (13) and (14), the power output and efficiency of the LD heat engine can be expressed as

$$P = \frac{W_e}{t_e} = \frac{(T_h - T_m)\Delta S_e}{t_e} - \frac{\alpha\Sigma_{me} + (1 - \alpha)\Sigma_h}{\alpha(1 - \alpha)t_e^2}, \quad \text{(B1)}$$

$$\eta = \frac{W_e}{Q_h} = \frac{\eta_C}{1 + T_m\Delta S_{\mathrm{tot,e}}/(Pt_e)}, \quad \text{(B2)}$$

where

$$\Delta S_{\mathrm{tot,e}} = -\frac{Q_h}{T_h} + \frac{Q_{me}}{T_m} = \frac{\Sigma_h}{t_h T_h} + \frac{\Sigma_{me}}{t_{me} T_m} \geqslant 0 \quad \text{(B3)}$$

is the total entropy production per engine cycle.

Maximizing the power (B1) with respect to α and t_e yields [15]

$$\alpha_e^* = \frac{\sqrt{\Sigma_e}}{1 + \sqrt{\Sigma_e}}, \quad \text{(B4)}$$

$$t_e^* = \frac{2(\sqrt{\Sigma_h} + \sqrt{\Sigma_{me}})^2}{T_h\eta_C\Delta S_e}, \quad \text{(B5)}$$

$$P^* = \frac{1}{4}\left(\frac{T_h\eta_C\Delta S_e}{\sqrt{\Sigma_h} + \sqrt{\Sigma_{me}}}\right)^2, \quad \text{(B6)}$$

$$\eta^* = \frac{\eta_C(1 + \sqrt{\Sigma_e})}{2 + \sqrt{\Sigma_e}(2 - \eta_C)}, \quad \text{(B7)}$$

where $\Sigma_e = \Sigma_h/\Sigma_{me}$ is the so-called irreversibility ratio and $\eta_C = 1 - T_m/T_h$ denotes Carnot efficiency. Now we use Eqs. (B4) and (B5) to define the coordinate transformation

$$\tau_e = \frac{t_e}{t_e^*} - 1 \in [-1, \infty], \quad \text{(B8)}$$

$$a = \frac{\alpha_e}{\alpha_e^*} - 1 \in \left[-1, \frac{1}{\alpha_e^*} - 1\right], \quad \text{(B9)}$$

which reduces the number of variables in the problem [25]. The point of maximum power (B6) corresponds to $\delta P = 0$ (17) and $\tau_e = a = 0$. The (relative) loss in power (17) and efficiency (B2) in these new coordinates read

$$\delta P = \frac{a^2\sqrt{\Sigma_e}}{(1 + a)(a\sqrt{\Sigma_e} - 1)(1 + \tau_e)^2} - \left(\frac{\tau_e}{1 + \tau_e}\right)^2, \quad \text{(B10)}$$

$$
\begin{aligned}
\eta = {}&\frac{(1 + \sqrt{\Sigma_e})\eta_C}{a\sqrt{\Sigma_e} - 1} \\
&\times \frac{2a^2\sqrt{\Sigma_e}(1 + \tau_e) + (a\sqrt{\Sigma_e} - a - 1)(1 + 2\tau_e)}{2(1 + a)(1 + \sqrt{\Sigma_e})(1 + \tau_e) - \eta_C\sqrt{\Sigma_e}}.
\end{aligned}
\quad \text{(B11)}
$$

Solving Eq. (B10) with respect to the dimensionless cycle duration τ_e, we find two roots

$$\tau_e = \frac{-\delta P}{1 + \delta P} \pm \frac{\sqrt{\delta P(1 + a - a\sqrt{\Sigma_e}) + a^2\sqrt{\Sigma_e}}}{(1 + \delta P)\sqrt{(1 + a)(a\sqrt{\Sigma_e} - 1)}}. \quad \text{(B12)}$$

Since longer cycles in general allow for larger efficiencies, we thus take the root with the positive sign. Substituting it into Eq. (B11), evaluating the condition $\partial\eta/\partial a|_{a=a^{\mathrm{opt}}} = 0$ for maximum efficiency, and expanding it up to the fourth order in a, we find

$$\left.\frac{\partial\eta}{\partial a}\right|_{a=a^{\mathrm{opt}}} = \sum_{n=0}^{4} b_n a^n + \mathcal{O}(a^5) = 0, \quad \text{(B13)}$$

where the coefficients b_n are complicated functions of δP, Σ_e, and η_C. Equation (B13) for the optimal value a^{opt} of the parameter a can be solved exactly [65]. The corresponding optimal value of τ_e^{opt} follows by substituting the resulting a^{opt} for a in Eq. (B12).

Substituting the obtained expressions for a^{opt} and τ_e^{opt} for a and τ into Eq. (B11), we obtain a lengthy but manageable (e.g., by using software for symbolic manipulation such as MATHEMATICA) formula for the MEGP for LD heat engines

$$\eta^{\mathrm{opt}} = \eta^{\mathrm{opt}}(\delta P, \Sigma_e, \eta_C). \quad \text{(B14)}$$

Even though this results was obtained using the approximation (B13), we tested that the resulting approximate MEGP (B14) and the exact MEGP obtained numerically are indistinguishable within the numerical precision (the measured absolute error is on the order of 10^{-7}). Furthermore, the expression (B14) yields exact lower ($\Sigma_e = 0$) and upper

$(\Sigma_e \to \infty)$ bounds on the MEGP of LD heat engines [25]

$$\frac{\eta_C}{2}(1 + \sqrt{-\delta P}) \leqslant \eta^{\text{opt}} \leqslant \frac{\eta_C(1 + \sqrt{-\delta P})}{2 - \eta_C(1 - \sqrt{-\delta P})}. \quad \text{(B15)}$$

APPENDIX C: MEGP FOR LD REFRIGERATORS

In this Appendix, we review the derivation of the expression ε^{opt} for MEGP for LD refrigerators given in Ref. [44].

The COP of the refrigerator is given by

$$\varepsilon = \frac{Q_c}{W_r} = \frac{\varepsilon_C}{1 + \varepsilon_C T_m \Delta S_{\text{tot,r}}/(Rt_r)}, \quad \text{(C1)}$$

where

$$\Delta S_{\text{tot,r}} = -\frac{Q_c}{T_c} + \frac{Q_{mr}}{T_m} = \frac{\Sigma_c}{t_c T_c} + \frac{\Sigma_{mr}}{t_{mr} T_m} \geqslant 0 \quad \text{(C2)}$$

is the total entropy production per refrigeration cycle. Substituting Eq. (15) into Eq. (4) and maximizing the resulting expression with respect to t_{mr} and t_c gives [44,66]

$$t_c^* = t_r^* = \frac{2\Sigma_c}{T_c \Delta S_r}, \quad \text{(C3)}$$

$$R^* = \frac{(T_c \Delta S_r)^2}{4\Sigma_c}. \quad \text{(C4)}$$

At maximum power conditions, the duration of the cold isotherm t_c^* thus equals the duration of the entire cycle t_r^*, which should be understood in the sense that the hot isotherm is infinitely faster than the cold one. The corresponding COP of the internal refrigerator at maximum power ε^* reads

$$\varepsilon_-^* = 0 \qquad \text{for} \quad \Sigma_r > 0, \quad \text{(C5)}$$

$$\varepsilon_+^* = \frac{\varepsilon_C}{2 + \varepsilon_C} \quad \text{for} \quad \Sigma_r = 0, \quad \text{(C6)}$$

where $\Sigma_r = \Sigma_{mr}/\Sigma_c$ is the so-called irreversibility ratio and $\varepsilon_C = T_c/(T_m - T_c)$ denotes Carnot COP. The COP at maximum power ε^* thus exhibits a discontinuity at $\Sigma_r = 0$. Using Eq. (C3), we define the dimensionless cycle duration as

$$\tau_r = \frac{t_r}{t_r^*} - 1 \in [-1, \infty]. \quad \text{(C7)}$$

Introducing further the relative duration of the hot isotherm $\alpha_r = t_{mr}/t_r$, we find from Eqs. (4), (17), and (C7) that

$$\alpha_r = 1 + \frac{1}{(1 + \delta R)\tau_r^2 + 2\delta R \tau_r + \delta R - 1}. \quad \text{(C8)}$$

Since α_r by definition satisfies $0 \leqslant \alpha_r \leqslant 1$, the above formula makes sense only if

$$-\frac{\sqrt{-\delta R}}{1 + \sqrt{-\delta R}} \leqslant \tau_r \leqslant \frac{\sqrt{-\delta R}}{1 - \sqrt{-\delta R}}. \quad \text{(C9)}$$

The COP (C1) in these new variables reads

$$\varepsilon = \frac{\tau_r^3 + A_{1,3}\tau_r^2 + A_{0,3}\tau_r + A_{0,1}}{-\tau_r^3 + A_{1/\varepsilon_+^*, -3}\tau_r^2 + B_{3,4,1}\tau_r + B_{1,2,-1}}, \quad \text{(C10)}$$

with $A_{k,l} = (k + l\delta R)/(1 + \delta R)$ and $B_{k,l,m} = [-k(\delta R)^2 + (l/\varepsilon_C + 1 + \Sigma_r)\delta R + m\Sigma_r]/(1 + \delta R)^2$. The maximum of COP (C10) can be determined by the condition $\partial \varepsilon/\partial \tau_r|_{\tau_r = \tau_r^{\text{opt}}} = 0$, which explicitly reads

$$(\tau_r^{\text{opt}})^4 + \tilde{A}(\tau_r^{\text{opt}})^3 + \tilde{B}_{6+3\tilde{\Sigma}_r, 2+2\tilde{\Sigma}_r, -\tilde{\Sigma}_r}(\tau_r^{\text{opt}})^2$$
$$+ \tilde{B}_{4+3\tilde{\Sigma}_r, -2\tilde{\Sigma}_r, -\tilde{\Sigma}_r}\tau_r^{\text{opt}} + \tilde{B}_{1+\tilde{\Sigma}_r, -2\tilde{\Sigma}_r, 0} = 0. \quad \text{(C11)}$$

Above, the coefficients $\tilde{A} = [(4 + \tilde{\Sigma}_r)\delta R + \tilde{\Sigma}_r]/(1 + \delta R)$ and $\tilde{B}_{k,l,m} = (k\delta R^2 + l\delta R + m)/(1 + \delta R)^2$ depend on Σ_r and ε_C only through the combination $\tilde{\Sigma}_r = \Sigma_r/(\frac{1}{\varepsilon_C} + 1)$.

The quartic equation (C11) has four roots and can be analytically solved [44,65]. The optimal dimensionless cycle duration $\tau_r^{\text{opt}} = \tau_r^{\text{opt}}(\delta R, \Sigma_r, \varepsilon_C)$ is determined by the only physically reasonable root, located in the interval (C9). Substituting it for τ in Eq. (C10), we obtain a lengthy but manageable (e.g., by using software for symbolic manipulation such as MATHEMATICA) exact expression for ε^{opt},

$$\varepsilon^{\text{opt}} = \varepsilon^{\text{opt}}(\delta R, \Sigma_r, \varepsilon_C). \quad \text{(C12)}$$

It turns out to be bounded by the inequalities

$$0 \leqslant \varepsilon^{\text{opt}} \leqslant \frac{\varepsilon_C(1 + \sqrt{-\delta R})}{2 + \varepsilon_C(1 - \sqrt{-\delta R})} \equiv \varepsilon_+^{\text{opt}}, \quad \text{(C13)}$$

where the lower bound corresponds to $\Sigma_r \to \infty$ and the upper bound to $\Sigma_r = 0$.

[1] H. B. Callen, *Thermodynamics and an Introduction to Thermostatistics*, Student Edition (Wiley India, Noida, India, 2006).

[2] V. Holubec and A. Ryabov, Diverging, but negligible power at carnot efficiency: Theory and experiment, Phys. Rev. E **96**, 062107 (2017).

[3] I. Müller, *A History of Thermodynamics: The Doctrine of Energy and Entropy* (Springer, New York, 2007).

[4] J. Yvon, Saclay reactor: Acquired knowledge by two years experience in heat transfer using compressed Gas, Tech. Rep. (CEA Saclay, Saclay, France, 1955).

[5] P. Chambadal, *Les Centrales Nucléaires*, Vol. 321 (Colin, Paris, 1957).

[6] I. I. Novikov, The efficiency of atomic power stations (a review), J. Nucl. Energy II **7**, 125 (1958).

[7] M. Esposito, R. Kawai, K. Lindenberg, and C. Van den Broeck, Efficiency at Maximum Power of Low-Dissipation Carnot Engines, Phys. Rev. Lett. **105**, 150603 (2010).

[8] J. Gonzalez-Ayala, J. Guo, A. Medina, J. M. M. Roco, and A. C. Hernández, Energetic Self-Optimization Induced by Stability in Low-Dissipation Heat Engines, Phys. Rev. Lett. **124**, 050603 (2020).

[9] Y. Wang, M. Li, Z. C. Tu, A. C. Hernández, and J. M. M. Roco, Coefficient of performance at maximum figure of merit and its

bounds for low-dissipation carnot-like refrigerators, Phys. Rev. E **86**, 011127 (2012).

[10] C. Van den Broeck, Thermodynamic Efficiency at Maximum Power, Phys. Rev. Lett. **95**, 190602 (2005).

[11] G. Benenti, K. Saito, and G. Casati, Thermodynamic Bounds on Efficiency for Systems with Broken Time-Reversal Symmetry, Phys. Rev. Lett. **106**, 230602 (2011).

[12] Y. Izumida and K. Okuda, Work Output and Efficiency at Maximum Power of Linear Irreversible Heat Engines Operating with a Finite-Sized Heat Source, Phys. Rev. Lett. **112**, 180603 (2014).

[13] Y. Izumida, K. Okuda, J. M. M. Roco, and A. C. Hernández, Heat devices in nonlinear irreversible thermodynamics, Phys. Rev. E **91**, 052140 (2015).

[14] Y. Izumida and K. Okuda, Efficiency at maximum power of minimally nonlinear irreversible heat engines, Europhys. Lett. **97**, 10004 (2012).

[15] T. Schmiedl and U. Seifert, Efficiency at maximum power: An analytically solvable model for stochastic heat engines, Europhys. Lett. **81**, 20003 (2007).

[16] D. Segal, Stochastic Pumping of Heat: Approaching the Carnot Efficiency, Phys. Rev. Lett. **101**, 260601 (2008).

[17] C. Jarzynski and O. Mazonka, Feynman's ratchet and pawl: An exactly solvable model, Phys. Rev. E **59**, 6448 (1999).

[18] M. Esposito, K. Lindenberg, and C. Van den Broeck, Universality of Efficiency at Maximum Power, Phys. Rev. Lett. **102**, 130602 (2009).

[19] M. Esposito, K. Lindenberg, and C. Van den Broeck, Thermoelectric efficiency at maximum power in a quantum dot, Europhys. Lett. **85**, 60010 (2009).

[20] M. Esposito, R. Kawai, K. Lindenberg, and C. Van den Broeck, Quantum-dot carnot engine at maximum power, Phys. Rev. E **81**, 041106 (2010).

[21] N. Nakpathomkun, H. Q. Xu, and H. Linke, Thermoelectric efficiency at maximum power in low-dimensional systems, Phys. Rev. B **82**, 235428 (2010).

[22] R. S. Whitney, Most Efficient Quantum Thermoelectric at Finite Power Output, Phys. Rev. Lett. **112**, 130601 (2014).

[23] R. S. Whitney, Finding the quantum thermoelectric with maximal efficiency and minimal entropy production at given power output, Phys. Rev. B **91**, 115425 (2015).

[24] V. Holubec and A. Ryabov, Efficiency at and near maximum power of low-dissipation heat engines, Phys. Rev. E **92**, 052125 (2015).

[25] V. Holubec and A. Ryabov, Maximum efficiency of low-dissipation heat engines at arbitrary power, J. Stat. Mech. (2016) 073204.

[26] A. Ryabov and V. Holubec, Maximum efficiency of steady-state heat engines at arbitrary power, Phys. Rev. E **93**, 050101(R) (2016).

[27] A. Dechant, N. Kiesel, and E. Lutz, Underdamped stochastic heat engine at maximum efficiency, Europhys. Lett. **119**, 50003 (2017).

[28] Y. Apertet, H. Ouerdane, A. Michot, C. Goupil, and P. Lecoeur, On the efficiency at maximum cooling power, Europhys. Lett. **103**, 40001 (2013).

[29] Z. Yan and J. Chen, A class of irreversible carnot refrigeration cycles with a general heat transfer law, J. Phys. D **23**, 136 (1990).

[30] C. de Tomás, A. C. Hernández, and J. M. M. Roco, Optimal low symmetric dissipation carnot engines and refrigerators, Phys. Rev. E **85**, 010104(R) (2012).

[31] A. C. Hernández, A. Medina, J. M. M. Roco, J. A. White, and S. Velasco, Unified optimization criterion for energy converters, Phys. Rev. E **63**, 037102 (2001).

[32] F. Angulo-Brown, An ecological optimization criterion for finite-time heat engines, J. Appl. Phys. **69**, 7465 (1991).

[33] Y. Izumida, K. Okuda, A. C. Hernández, and J. Roco, Coefficient of performance under optimized figure of merit in minimally nonlinear irreversible refrigerator, Europhys. Lett. **101**, 10005 (2013).

[34] C. de Tomas, J. M. M. Roco, A. C. Hernández, Y. Wang, and Z. C. Tu, Low-dissipation heat devices: Unified trade-off optimization and bounds, Phys. Rev. E **87**, 012105 (2013).

[35] N. Sánchez-Salas, L. López-Palacios, S. Velasco, and A. Calvo Hernández, Optimization criteria, bounds, and efficiencies of heat engines, Phys. Rev. E **82**, 051101 (2010).

[36] Y. Zhang, C. Huang, G. Lin, and J. Chen, Universality of efficiency at unified trade-off optimization, Phys. Rev. E **93**, 032152 (2016).

[37] R. Long and W. Liu, Ecological optimization for general heat engines, Phys. A: Stat. Mech. Appl. **434**, 232 (2015).

[38] V. Blickle and C. Bechinger, Realization of a micrometre-sized stochastic heat engine, Nat. Phys. **8**, 143 (2012).

[39] I. A. Martínez, É. Roldán, L. Dinis, D. Petrov, J. M. Parrondo, and R. A. Rica, Brownian carnot engine, Nat. Phys. **12**, 67 (2016).

[40] K. Sekimoto and S.-I. Sasa, Complementarity relation for irreversible process derived from stochastic energetics, J. Phys. Soc. Jpn. **66**, 3326 (1997).

[41] P. R. Zulkowski and M. R. DeWeese, Optimal protocols for slowly driven quantum systems, Phys. Rev. E **92**, 032113 (2015).

[42] V. Cavina, A. Mari, and V. Giovannetti, Slow Dynamics and Thermodynamics of Open Quantum Systems, Phys. Rev. Lett. **119**, 050601 (2017).

[43] Y.-H. Ma, R.-X. Zhai, J. Chen, C. P. Sun, and H. Dong, Experimental Test of the $1/\tau$-Scaling Entropy Generation in Finite-Time Thermodynamics, Phys. Rev. Lett. **125**, 210601 (2020).

[44] V. Holubec and Z. Ye, Maximum efficiency of low-dissipation refrigerators at arbitrary cooling power, Phys. Rev. E **101**, 052124 (2020).

[45] J. Guo, H. Yang, H. Zhang, J. Gonzalez-Ayala, J. Roco, A. Medina, and A. C. Hernández, Thermally driven refrigerators: Equivalent low-dissipation three-heat-source model and comparison with experimental and simulated results, Energy Convers. Manag. **198**, 111917 (2019).

[46] J. Guo, H. Yang, J. Gonzalez-Ayala, J. Roco, A. Medina, and A. C. Hernández, The equivalent low-dissipation combined cycle system and optimal analyses of a class of thermally driven heat pumps, Energy Convers. Manag. **220**, 113100 (2020).

[47] A. Levy and R. Kosloff, Quantum Absorption Refrigerator, Phys. Rev. Lett. **108**, 070604 (2012).

[48] L. A. Correa, J. P. Palao, G. Adesso, and D. Alonso, Performance bound for quantum absorption refrigerators, Phys. Rev. E **87**, 042131 (2013).

[49] L. A. Correa, J. P. Palao, D. Alonso, and G. Adesso, Quantum-enhanced absorption refrigerators, Sci. Rep. **4**, 3949 (2014).

[50] J. B. Brask and N. Brunner, Small quantum absorption refrigerator in the transient regime: Time scales, enhanced cooling, and entanglement, Phys. Rev. E **92**, 062101 (2015).

[51] J. O. González, J. P. Palao, and D. Alonso, Relation between topology and heat currents in multilevel absorption machines, New J. Phys. **19**, 113037 (2017).

[52] V. Holubec and T. Novotný, Effects of noise-induced coherence on the fluctuations of current in quantum absorption refrigerators, J. Chem. Phys. **151**, 044108 (2019).

[53] G. Maslennikov, S. Ding, R. Hablützel, J. Gan, A. Roulet, S. Nimmrichter, J. Dai, V. Scarani, and D. Matsukevich, Quantum absorption refrigerator with trapped ions, Nat. Commun. **10**, 202 (2019).

[54] One might argue that, when operating simultaneously, the internal heat engine cannot power the internal refrigerator because the engine generates work during half of the cycle only and accepts it during the rest. However, already the realization of a cyclically operating heat engine requires the existence of a work source, where the work generated by the engine is stored and which is used to propel the engine during parts of the cycle where it accepts energy. The same work source can power the simultaneous CAR. In practice, the energy transfer to/from the work source could lead to additional losses decreasing the performance of the CAR. Since our aim here is to provide an upper bound on efficiency, we neglect such losses. Furthermore, we are interested only on second law limitations on the performance of the CAR working under idealistic conditions (no heat leakages, no losses during work-to-work conversion) and thus the practical implementation of the work source is irrelevant for our analysis.

[55] R. Long, Z. Liu, and W. Liu, Performance analysis for minimally nonlinear irreversible refrigerators at finite cooling power, Phys. A: Stat. Mech. Appl. **496**, 137 (2018).

[56] R. Long and W. Liu, Efficiency and its bounds of minimally nonlinear irreversible heat engines at arbitrary power, Phys. Rev. E **94**, 052114 (2016).

[57] Adiabatic processes are described by vanishing average heat flux into the system and can be realized either by disconnecting the system from the thermal environment or by changing the control parameters in such a way that the average heat flux vanishes [39,67]. A fast adiabat is effectively an example

of the first case since the heat does not have enough time to enter the system, see Ref. [38] for an experimental realization of such branches in an over-damped Brownian setup. In general, fast changes of control parameters can bring the system far from equilibrium. In the overdamped description, this can be avoided by suitably tuning the jump in potential and temperature [15,24]. However, in the underdamped regime this is in general not possible and one has to employ adiabatic branches with finite duration. In our present analysis, this would lead to a decrease in output power of all the considered devices.

[58] P. Abiuso and M. Perarnau-Llobet, Optimal Cycles for Low-Dissipation Heat Engines, Phys. Rev. Lett. **124**, 110606 (2020).

[59] P. Abiuso, H. J. D. Miller, M. Perarnau-Llobet, and M. Scandi, Geometric optimisation of quantum thermodynamic processes, Entropy **22**, 1076 (2020).

[60] I. Reyes-Ramírez, J. Gonzalez-Ayala, A. Calvo Hernández, and M. Santillán, Local-stability analysis of a low-dissipation heat engine working at maximum power output, Phys. Rev. E **96**, 042128 (2017).

[61] J. Gonzalez-Ayala, M. Santillán, I. Reyes-Ramírez, and A. Calvo-Hernández, Link between optimization and local stability of a low-dissipation heat engine: Dynamic and energetic behaviors, Phys. Rev. E **98**, 032142 (2018).

[62] J. Gonzalez-Ayala, J. Guo, A. Medina, J. M. M. Roco, and A. Calvo Hernández, Optimization induced by stability and the role of limited control near a steady state, Phys. Rev. E **100**, 062128 (2019).

[63] F. L. Curzon and B. Ahlborn, Efficiency of a carnot engine at maximum power output, Am. J. Phys. **43**, 22 (1975).

[64] Z.-C. Tu, Recent advance on the efficiency at maximum power of heat engines, Chin. Phys. B **21**, 020513 (2012).

[65] M. Abramowitz and I. A. Stegun, *Handbook of Mathematical Functions with Formulas, Graphs, and Mathematical Tables*, Vol. 55 (Dover, New York, 1964).

[66] A. C. Hernández, A. Medina, and J. Roco, Time, entropy generation, and optimization in low-dissipation heat devices, New J. Phys. **17**, 075011 (2015).

[67] I. A. Martínez, E. Roldán, L. Dinis, D. Petrov, and R. A. Rica, Adiabatic Processes Realized with a Trapped Brownian Particle, Phys. Rev. Lett. **114**, 120601 (2015).